

A New Approach to Motion Modeling and Autopilot Design of Skid-To-Turn Missiles

Chanho Song, Yoon-Sik Kim

Abstract: In this paper, we present a new approach to autopilot design for skid-to-turn missiles which may have severe aerodynamic cross-couplings and nonlinearities with angle of attack. The model of missile motion is derived in the maneuver plane and, based on that model, pitch, yaw, and roll autopilot are designed. They are composed of a nonlinear term which compensates for the aerodynamic couplings and nonlinearities and a linear controller driven by the measured outputs of missile accelerations and angular rates. Besides the outputs, further information such as Mach number, dynamic pressure, total angle of attack, and bank angle is required. With the proposed autopilot and simple estimators of bank angle and total angle of attack, it is shown by computer simulations that the induced moments and some aerodynamic nonlinearities are properly compensated and that the performance is superior to that of the conventional ones.

Keywords: autopilot, missile modeling, aerodynamic coupling, skid-to-turn missiles, bank angle estimator

I. Introduction

In general, autopilots for STT(Skid-To-Turn) missiles are designed based on the assumption that cross-couplings among roll, pitch, and yaw channels are negligible.[1] However, this assumption is valid if the system works at low angle of attack. There may be large aerodynamic couplings among these channels due to the bank angle which varies with the target maneuver. This aerodynamic coupling comprises a dynamic interchannel coupling mode, and the maintenance of stability becomes increasingly more difficult as missile angle of attack is increased. Among strategies used so far to reduce these coupling effects, the following two ones seem to be prevalent. The one is to limit, to some extent, the total angle of attack because the aerodynamic couplings and nonlinearities increase with the angle of attack, and the other is to select smaller bandwidths of pitch and yaw loops than that of the roll loop. However, these methods are not optimal solutions because the former limits the maneuverability and the latter can make the response of the pitch(or yaw) loop sluggish.[2]

Not only the design methodology but also the structure of the autopilot is worth noting. In case that the missile configuration is symmetric cruciform, the structure of yaw autopilot is usually made to be the same as the pitch autopilot, but with this structure it is difficult to take the so-called induced yawing force and moment into consideration in the autopilot design. As well known, even if the configuration of airframe has symmetry, the air flow about the maneuver plane may be asymmetric, and such undesired forces and moments can be induced in the direction perpendicular to the maneuver plane. Another aspect of common pitch (or yaw) autopilots is that control parameters are not implemented as a function of angle of attack, though aerodynamics may be heavily nonlinear with the angle of attack, especially for the highly maneuverable missiles.

In this paper, we present a new approach to autopilot design for STT missiles which may have severe aerodynamic cross-couplings and nonlinearities with angle of attack. First, we

derive the missile motion model where the aerodynamic characteristics of STT missiles are well delineated. Based on this model, we design pitch, yaw, and roll autopilot which are composed of a nonlinear term which compensates for the aerodynamic couplings and nonlinearities and a linear controller driven by the measured outputs of missile accelerations and angular rates. Besides the outputs, the proposed autopilot requires further information such as Mach number, dynamic pressure, total angle of attack, and bank angle. Among those, the first two parameters are used for the gain-scheduling, and the rest for the compensation of couplings and nonlinearities. In case that bank angle and angle of attack are not measurable, which commonly happens in practice, estimators ought to be designed. With the proposed autopilot and simple estimators of bank angle and total angle of attack, it is shown by computer simulations that the induced moments and some aerodynamic nonlinearities are properly compensated and that the performance is superior to that of the conventional ones.

II. Coordinate frames

In this section, we define several coordinate frames necessary for the motion modeling. Let X_b, Y_b and Z_b be the reference axes of the missile body frame as in Fig. 1. Denoting the transformation matrix to the rotation about i axis, $i = x, y, z$ through the angle θ by $[\theta]_i$, then the maneuver frame is defined as the one transformed from the body frame by $[-\Gamma]_x$, where Γ is the bank angle. Rotating again the maneuver frame about the Y_m axis through the total angle of attack, $-\alpha_t$, we get the wind frame. The X_w axis of the wind frame comes into coincidence with the missile velocity vector.

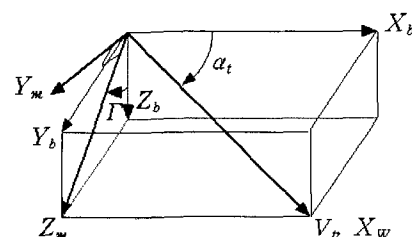


Fig. 1. Illustration of coordinate systems.

Manuscript received: Dec. 10, 2001, Accepted: Apr. 8, 2002.

Chanho Song, Yoon-Sik Kim: Agency for Defense Development
P.O.Box 35-3, Yuseong, Daejeon, 305-600, Korea.(chsong@add.
re.kr, wontwoo@hananet.net)

Let V^b , V^m , and V^w be a vector represented in the body, maneuver, and wind coordinates, respectively. Then the relationship between the frames can be depicted as follows :

$$V^b \rightarrow V^m \rightarrow V^w$$

$$[-\Gamma]_x \quad [-\alpha_i]_y$$

We introduce another notation C_i^j for the transformation matrix from the i frame to the j frame.

$$C_b^m = [-\Gamma]_x = \begin{bmatrix} 1 & 0 & 0 \\ 0 & C\Gamma & -S\Gamma \\ 0 & S\Gamma & C\Gamma \end{bmatrix} \quad (1)$$

$$C_m^w = [-\alpha_i]_y = \begin{bmatrix} C\alpha_i & 0 & S\alpha_i \\ 0 & 1 & 0 \\ -S\alpha_i & 0 & C\alpha_i \end{bmatrix} \quad (2)$$

$$C_b^w = C_m^w C_b^m = \begin{bmatrix} C\alpha_i & S\alpha_i S\Gamma & S\alpha_i C\Gamma \\ 0 & C\Gamma & -S\Gamma \\ -S\alpha_i & C\alpha_i S\Gamma & C\alpha_i C\Gamma \end{bmatrix} \quad (3)$$

where S and C are the abbreviations of sine and cosine, respectively.

III. Modeling for the cruciform missiles

In this section, we derive the motion model of the cruciform missiles. The following somewhat standard assumptions are used in the derivation.

Assumption 1 : The effect of gravity is neglected.

Assumption 2 : Thrust force is exhausted and velocity and mass of the missile are constant.

Assumption 3 : Contributions of the main wing and control fins to the moment of inertia and product of inertia are negligible.

Assumption 1 and 2 mean that there are no applied forces to the missile but the aerodynamic forces.

We now set up the force equations in the wind frame. From the standard results (for example, [3]), force equations can be expressed as follows:

$$F_{xw} = m(\dot{U}_w + q_w W_w - r_w V_w) \quad (4)$$

$$F_{yw} = m(\dot{V}_w + r_w U_w - p_w W_w) \quad (5)$$

$$F_{zw} = m(\dot{W}_w + p_w V_w - q_w U_w) \quad (6)$$

where m is the missile mass and subscript w represents that coordinates. In the wind frame, V_w , W_w , \dot{V}_w and \dot{W}_w are all zero, and U_w is equal to the total velocity, V_t , so we get

$$\dot{V}_t = (F_{xm} \cos \alpha_i + F_{zm} \sin \alpha_i) / m \quad (7)$$

$$r_w = F_{ym} / (mV_t) \quad (8)$$

$$q_w = -(-F_{xm} \sin \alpha_i + F_{zm} \cos \alpha_i) / (mV_t) \quad (9)$$

In the above equations, subscript m represents the maneuver coordinates. Since the missile velocity is assumed to be constant in Assumption 2, Eq. (7) is meaningless.

Before deriving the moment equations, we further introduce a notation ω_{ik}^l which means the angular rate of the k frame with respect to the inertial frame i represented in the l frame. With the notation, we have

$$\omega_{im}^m = \begin{bmatrix} p_m \\ q_m \\ r_m \end{bmatrix} = C_b^m \begin{bmatrix} p_b \\ q_b \\ r_b \end{bmatrix} + \begin{bmatrix} -\dot{\Gamma} \\ 0 \\ 0 \end{bmatrix} = \begin{bmatrix} p_b - \dot{\Gamma} \\ q_b C\Gamma - r_b S\Gamma \\ q_b S\Gamma + r_b C\Gamma \end{bmatrix} \quad (10)$$

$$\omega_{iw}^w = \begin{bmatrix} p_w \\ q_w \\ r_w \end{bmatrix} = C_m^w \begin{bmatrix} p_m \\ q_m \\ r_m \end{bmatrix} + \begin{bmatrix} 0 \\ -\dot{\alpha}_i \\ 0 \end{bmatrix} = \begin{bmatrix} p_m C\alpha_i + r_m S\alpha_i \\ q_m - \dot{\alpha}_i \\ -p_m S\alpha_i + r_m C\alpha_i \end{bmatrix} \quad (11)$$

Then, from Eqs. (9) and (10),

$$\dot{\alpha}_i = q_m - q_w = q_m + (-F_{xm} \sin \alpha_i + F_{zm} \cos \alpha_i) / (mV_t) \quad (12)$$

Furthermore, from Eqs. (8), (10), and (11),

$$\dot{\Gamma} = p_b - p_m = p_b + (r_w - r_m \cos \alpha_i) / \sin \alpha_i \\ = p_b + (F_{ym} / (mV_t) - r_m \cos \alpha_i) / \sin \alpha_i \quad (13)$$

When I^m is the inertia dyadic in the maneuver frame, let

$$I^m = \begin{bmatrix} I_x & -I_{xy} & -I_{xz} \\ -I_{xy} & I_y & -I_{xz} \\ -I_{xz} & -I_{xz} & I_z \end{bmatrix}$$

Then, it follows from Assumption 3 that I^m is constant regardless of Γ , $I^m = I^b$, $I_y = I_z$, and $I_{xy} = I_{xz} = I_{yz} = 0$. Denoting the moment applied to the missile in the maneuver coordinates as M^m then we have from reference [4, 5],

$$M^m = C_i^m M^i = C_i^m \frac{d}{dt} (C_m^i I^m \omega_{ib}^m) = C_i^m (\dot{C}_m^i I^m \omega_{ib}^m + C_m^i I^m \dot{\omega}_{ib}^m) \\ = C_i^m (C_m^i \Omega_{im}^m I^m \omega_{ib}^m + C_m^i I^m \dot{\omega}_{ib}^m)$$

where Ω_{im}^m is the skew symmetry matrix of a vector ω_{im}^i , i.e.,

$$\Omega_{im}^m = \begin{bmatrix} 0 & -r_m & q_m \\ r_m & 0 & -p_m \\ -q_m & p_m & 0 \end{bmatrix} \quad \text{for } \omega_{im}^m = \begin{bmatrix} p_m \\ q_m \\ r_m \end{bmatrix}.$$

Since $\omega_{ib}^m = \omega_{im}^m + \omega_{mb}^m = \begin{bmatrix} p_m + \dot{\Gamma} \\ q_m \\ r_m \end{bmatrix}$ and $p_m + \dot{\Gamma} = p_b$ from Eq. (13),

$$M^m = \begin{bmatrix} I_x & 0 & 0 \\ 0 & I_y & 0 \\ 0 & 0 & I_z \end{bmatrix} \begin{bmatrix} \dot{p}_b \\ \dot{q}_b \\ \dot{r}_b \end{bmatrix} + \begin{bmatrix} 0 & -r_m & q_m \\ r_m & 0 & -p_m \\ -q_m & p_m & 0 \end{bmatrix} \begin{bmatrix} I_x & 0 & 0 \\ 0 & I_y & 0 \\ 0 & 0 & I_z \end{bmatrix} \begin{bmatrix} p_m \\ q_m \\ r_m \end{bmatrix} \\ = \begin{bmatrix} I_x \dot{p}_b \\ I_y \dot{q}_b + I_x r_m p_b - I_y (p_b - \dot{\Gamma}) r_m \\ I_y \dot{r}_b - I_x q_m p_b + I_y (p_b - \dot{\Gamma}) q_m \end{bmatrix} \quad \square$$

Let $M^m = (M_{xm}, M_{ym}, M_{zm})$. Then we finally get

$$\dot{p}_b = \frac{1}{I_x} M_{xm} \quad (14)$$

$$\dot{q}_m = \frac{1}{I_y} M_{ym} - \frac{I_x}{I_y} r_m p_b + (p_b - \dot{\Gamma}) r_m \quad (15)$$

$$\dot{r}_m = \frac{1}{I_z} M_{zm} - \frac{I_x}{I_y} q_m p_b + (p_b - \dot{\Gamma}) q_m \quad (16)$$

Now we formulate the applied moment and force terms, that is (F_{xm}, F_{ym}, F_{zm}) and (M_{xm}, M_{ym}, M_{zm}) , so that they can be used effectively in autopilot design. It is well known that aerodynamic forces and moments are functions of bank angle Γ , total angle of attack α_t , Mach number, n , dynamic pressure, Q , and control fin deflections. Consider the control fin deflections $(\delta_p, \delta_r, \delta_q)$ in the maneuver coordinates transformed from the body coordinates $(\delta_x, \delta_y, \delta_z)$ via the transformation

$$\begin{bmatrix} \delta_p \\ \delta_r \\ \delta_q \end{bmatrix} = C_b^m \begin{bmatrix} \delta_x \\ \delta_y \\ \delta_z \end{bmatrix} \quad (17)$$

We shall use $(\delta_p, \delta_r, \delta_q)$ instead of the actual fin deflections $(\delta_x, \delta_y, \delta_z)$. Now, based on the available aerodynamic data, we make another assumption.

Assumption 4: The control cross-couplings of $(\delta_p, \delta_r, \delta_q)$ are negligible.

Furthermore, contributions of the fin deflections $(\delta_p, \delta_r, \delta_q)$ and the missile main body to the aerodynamics are decomposed.

With this assumption, aerodynamic forces and moments can be written as follows.

$$\begin{aligned} F_{xm} &= QSC_x(n, \alpha_t, \Gamma, \delta_r, \delta_q), \\ C_x &= C_{x0}(n, \alpha_t, \Gamma) + C_{x1}(n, \alpha_t, \Gamma, \delta_r, \delta_q) \\ F_{ym} &= QSC_y(n, \alpha_t, \Gamma, \delta_r) \\ C_y &= C_{y0}(n, \alpha_t, \Gamma) + C_{y1}(n, \alpha_t, \Gamma, \delta_r) \\ F_{zm} &= QSC_z(n, \alpha_t, \Gamma, \delta_q) \\ C_z &= C_{z0}(n, \alpha_t, \Gamma) + C_{z1}(n, \alpha_t, \Gamma, \delta_q) \quad (18) \\ M_{xm} &= QSD(C_l(n, \alpha_t, \Gamma, \delta_p) + \frac{d}{2V_t} C_{lp} p_b) \\ C_l &= C_{l0}(n, \alpha_t, \Gamma) + C_{l1}(n, \alpha_t, \Gamma, \delta_p) \\ M_{ym} &= QSD(C_m(n, \alpha_t, \Gamma, \delta_q) + \frac{d}{2V_t} C_{mq} q_m) \\ C_m &= C_{m0}(n, \alpha_t, \Gamma) + C_{m1}(n, \alpha_t, \Gamma, \delta_q) \\ M_{zm} &= QSD(C_n(n, \alpha_t, \Gamma, \delta_r) + \frac{d}{2V_t} C_{nr} r_m) \\ C_n &= C_{n0}(n, \alpha_t, \Gamma) + C_{n1}(n, \alpha_t, \Gamma, \delta_r) \end{aligned}$$

where $C_i, i = x, y, z, l, m, n$ are the nondimensional stability derivatives, and C_{lp}, C_{mq} , and C_{nr} are the damping coefficients which are functions of Mach number, and S and d are the missile reference area and length, respectively. Summarizing the equations derived so far, we end up with

$$\dot{\alpha}_t = q_m + \frac{QS}{mV_t} (-C_x \sin \alpha_t + C_z \cos \alpha_t) \quad (19)$$

$$\dot{\Gamma} = p_b + \left(\frac{QS}{mV_t} C_y - r_m \cos \alpha_t \right) / \sin \alpha_t \quad (20)$$

$$\dot{q}_m = \frac{QSD}{I_y} C_m + M_q q_m - \frac{I_x}{I_y} r_m p_b + (p_b - \dot{\Gamma}) r_m \quad (21)$$

$$\dot{r}_m = \frac{QSD}{I_y} C_n + N_r r_m + \frac{I_x}{I_y} q_m p_b - (p_b - \dot{\Gamma}) q_m \quad (22)$$

$$\dot{p}_b = \frac{QSD}{I_x} C_l + L_p p_b \quad (23)$$

$$\text{where } M_q = \frac{QSD^2}{2I_y V_t} C_{mq}, N_r = \frac{QSD^2}{2I_y V_t} C_{nr}, \text{ and } L_p = \frac{QSD^2}{2I_x V_t} C_{lp}.$$

IV. Autopilot design

In this section, we present a design technique for the pitch, yaw, and roll autopilot based on the above motion model. Autopilot design for cruciform missile typically have been based on the use of three independent channel for pitch, yaw and roll, and each channel are fixed in body frame. Actuator command also determined in the frame using the body angular rates and normal accelerations. But in this paper, the maneuver in X - Z plane and in X - Y plane of the maneuver frame will be defined as the pitch motion and the yaw motion, respectively. The rotational motion about the X_b axis is defined to be the roll motion as usual. Now, we assume that missile accelerations and angular rates, Mach number and height are measurable. The design goal is to make missile follow the acceleration commands quickly and accurately.

1. Pitch and yaw autopilots

Assuming $p_b = 0$ and neglecting two terms, $C_x \sin \alpha_t$ and $r_m(p - \dot{\Gamma})$, from the Eqs. (19) and (21), we get

$$\begin{aligned} \dot{\alpha}_t &\approx q_m + \frac{QS}{mV_t} C_z \\ &= q_m + \frac{QS}{mV_t} (C_{z0}(n, \alpha_t, \Gamma) + C_{z1}(n, \alpha_t, \Gamma, \delta_q)) \quad (24) \end{aligned}$$

$$\dot{q}_m = \frac{QSD}{I_y} (C_{m0}(n, \alpha_t, \Gamma) + C_{m1}(n, \alpha_t, \Gamma, \delta_q)) + M_q q_m \quad (25)$$

For the cruciform missiles, C_{z0} can be expressed in terms of f_1 and f_2 which are functions of Mach number and total angle of attack as follows[6]:

$$C_{z0} = f_1(n, \alpha_t) + f_2(n, \alpha_t) \cos 4\Gamma \quad (26)$$

Now, we further simplify the aerodynamic model so that it can be used more effectively in autopilot design.

Assumption 5: C_{y1} and C_{z1} are not affected by Γ and linear to δ_r and δ_q respectively.

Assumption 6: C.g. and c.p. are located on the center line of the missile body, i.e., on the X axis of the body frame.

By Assumption 5, C_{z1} can be written as

$$C_{z1} = f_3(n, \alpha_t) \delta_q. \quad (27)$$

Furthermore, Assumption 6 leads C_{m0} and C_{m1} to the same form as Eqs. (26) and (27), respectively, i.e., for the certain functions g_1 , g_2 and g_3 ,

$$C_{m0} = g_1(n, \alpha_t) + g_2(n, \alpha_t) \cos 4\Gamma \quad (28)$$

$$C_{m1} = g_3(n, \alpha_t) \delta_q \quad (29)$$

Denoting the static margin, i.e., the distance from c.g. to c.p. as l_x and the distance from c.g. to the control fin position as l_c then the following equations hold :

$$g_1 = \frac{l_x}{d} f_1, \quad g_2 = \frac{l_x}{d} f_2, \quad \text{and} \quad g_3 = \frac{l_x}{d} f_3.$$

Inserting Eqs. (26) and (27) into equation (24), and Eqs. (28) and (29) into Eq. (25), we get

$$\dot{\alpha}_t = q_m + \frac{QS}{mV_t} (f_1 + f_2 \cos 4\Gamma + f_3 \delta_q) \quad (30)$$

$$\dot{q}_m = \frac{QSd}{I_y} (g_1 + g_2 \cos 4\Gamma + g_3 \delta_q) + M_q q_m \quad (31)$$

We now introduce a new input variable δ_{q1} such that

$$\delta_q = \delta_{q1} - \frac{g_2}{g_3} \cos 4\Gamma. \quad (32)$$

Inserting Eq. (32) into Eq. (31) gives

$$\dot{q}_m = \frac{QSd}{I_y} (g_1 + g_2 \delta_{q1}) + M_q q_m. \quad (33)$$

Substituting Eq. (32) for δ_q in Eq. (30) and using the fact that $|l_x/l_c| \ll 1$, we get

$$\dot{\alpha}_t = q_m + \frac{QS}{mV_t} (f_1 + f_2 \cos 4\Gamma + f_3 \delta_{q1}) \quad (34)$$

We now linearize Eqs. (33) and (34) about the trim conditions. The linearized equations will be used to design the linear control part. These equations have the following forms:

$$\Delta \alpha_t = \Delta q_m + Z_\alpha \Delta \alpha_t + Z_\delta \Delta \delta_{q1} + Z_r \Delta \Gamma \quad (35)$$

$$\Delta \dot{q}_m = M_\alpha \Delta \alpha_t + M_\delta \Delta \delta_{q1} + M_q \Delta q_m \quad (36)$$

In the above equations, the variables with Δ mean the perturbation variables and dimensional derivatives such as Z_α and M_α are given by

$$Z_\alpha = \frac{QS}{mV_t} \left(\frac{\partial f_1}{\partial \alpha_t} + \frac{\partial f_2}{\partial \alpha_t} \cos 4\Gamma + \frac{\partial f_3}{\partial \alpha_t} \delta_q \right),$$

$$M_\alpha = \frac{QSd}{I_y} \left(\frac{\partial g_1}{\partial \alpha_t} + \frac{\partial g_2}{\partial \alpha_t} \cos 4\Gamma + \frac{\partial g_3}{\partial \alpha_t} \delta_q \right),$$

$$Z_\delta = \frac{QS}{mV_t} f_3, \quad M_\delta = \frac{QSd}{I_y} g_3, \quad \text{and} \quad Z_r = -\frac{4QS}{mV_t} \sin 4\Gamma.$$

We take the pitch autopilot structure shown in Fig. 2. In Fig. 2, $\hat{\Gamma}$ is the estimated bank angle. Except for the path of $\cos 4\hat{\Gamma} K_{\delta q}$, this is due to Nesline[7].

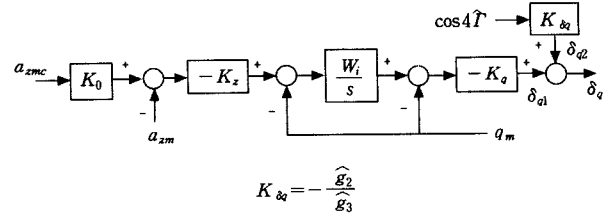


Fig. 2. Pitch autopilot structure.

On the other hand, from the Eq. (24),

$$a_{zn} = (\dot{\alpha}_t - q_m) V_t \quad (37)$$

which gives a perturbed equation about Δa_{zn} as follows :

$$\Delta a_{zn} = (\Delta \dot{\alpha}_t - \Delta q_m) V_t \quad (38)$$

We now consider the yaw motion. In yaw motion, C_{y0} is written as [6]

$$C_{y0} = f_4(n, \alpha_t) \sin 4\Gamma. \quad (39)$$

Then, similar to the pitch case, it follows from Assumption 5 and 6 that

$$C_{y1} = f_5(n, \alpha_t) \delta_r \quad (40)$$

$$C_{n0} = f_4(n, \alpha_t) \sin 4\Gamma \quad (41)$$

$$C_{n1} = g_5(n, \alpha_t) \delta_r \quad (42)$$

Furthermore, f_4 , f_5 and g_4 , g_5 satisfy the following relationship:

$$g_4 = -\frac{l_x}{d} f_4, \quad g_5 = -\frac{l_x}{d} f_5$$

Inserting Eqs. (39)~(42) into Eqs. (20) and (22), and neglecting the terms $q_m p_b$ and $(p_b - \dot{\Gamma}) q_m$, we get

$$\dot{\Gamma} = \frac{QS}{mV_t} (f_4 \sin 4\Gamma + f_5 \delta_r) / \sin \alpha_t - r \cot \alpha_t \quad (43)$$

$$\dot{r}_m = \frac{QSd}{I_y} (g_4 \sin 4\Gamma + g_5 \delta_r) + N_r r_m \quad (44)$$

As in the pitch case, we introduce a new variable δ_{r1} such that

$$\delta_r = \delta_{r1} - \frac{g_4}{g_5} \sin 4\Gamma \quad (45)$$

Inserting Eq. (45) into (44) yields

$$\dot{r}_m = \frac{QSd}{I_y} g_5 \delta_{r1} + N_r r_m \quad (46)$$

Substituting Eq. (45) for δ_r in Eq. (43) and using again the fact that $|l_x/l_c| \ll 1$, we have

$$\dot{\Gamma} = \frac{QS}{mV_t} (f_4 \sin 4\Gamma + f_5 \delta_{r1}) / \sin \alpha_t - r_m \cot \alpha_t \quad (47)$$

Linearization procedure is similar to the pitch case and we finally get the equations in the form of

$$\Delta \hat{\Gamma} = Y_a \Delta \alpha_i + Y_r \Delta \Gamma + Y_s \Delta \delta_{r1} \quad (48)$$

$$\Delta \dot{r}_m = N_r \Delta r_m + N_a \Delta \alpha_i + N_s \Delta \delta_{r1} \quad (49)$$

The structure of yaw autopilot is taken to be a simple rate loop as shown in Fig. 3 where yaw rate command is always given by 0.

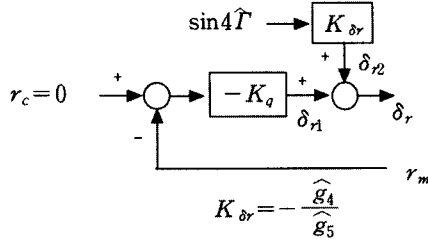


Fig. 3. Yaw autopilot structure.

Parameters of the linear control part in pitch and yaw autopilot can be determined by using design tools for the linear control systems and the linearized model derived above. Moreover, these control parameters are mostly scheduled in appropriate ways to cope with the wide variation of flight conditions. In this study, K_a, W_i, K_q and K_r were scheduled by Mach number, height, and $K_{\delta_q}, K_{\delta_r}$ and K_z were scheduled by Mach number, height, and total angle of attack.

The rationale of nonlinear terms in the autopilot is self-evident. $K_{\delta_q} \cos 4\hat{\Gamma}$ in the yaw autopilot compensates for the variation of aerodynamic nonlinearities due to the variation of bank angle and $K_{\delta_r} \sin 4\hat{\Gamma}$ in the yaw autopilot compensates for the induced yawing moment.

Now consider the estimators of bank angle and total angle of attack. Design problem of these estimators is not our concern. We consider simple estimators here. For the estimation of the bank angle, we shall use the following two forms :

$$\hat{\Gamma} = \tan^{-1} \left(\frac{-a_{ycb}}{-a_{zcb}} \right) \quad (50)$$

$$\hat{\Gamma}_c = \tan^{-1} \left(\frac{-a_{yc}}{-a_{zc}} \right) \quad (51)$$

where a_{ycb} and a_{zcb} are the missile acceleration in the body coordinates, and a_{yc} and a_{zc} are the acceleration commands in the same coordinates. Major difference between $\hat{\Gamma}$ and $\hat{\Gamma}_c$ is that the former has phase-lag compared to the true value while the latter has phase-lead. So, it seems desirable to mix them properly. Practical application will be shown later. For the estimation of total angle of attack, we shall make use of the table which stores the data of total angle of attack vs. pitch acceleration.

2. Roll autopilots

Similar to the yaw case, C_l can be written in the form

$$C_l = g_6(n, a_i) \sin 4\Gamma + g_7(n, a_i) \delta_p \quad (52)$$

where $g_6 \sin 4\Gamma$ represents the induced roll moment.

As in the pitch and yaw case, we introduce a new input variable δ_{p1} such that

$$\delta_p = \delta_{p1} - \frac{g_6}{g_7} \sin 4\Gamma \quad (53)$$

Inserting Eqs. (52), (53) into Eq. (23) and linearizing the resultant, we get

$$\Delta \dot{p}_b = L_p \Delta p_b + L_\delta \delta_p + L_a \Delta a_i \quad (54)$$

Roll autopilot structure is selected as shown in Fig. 4.

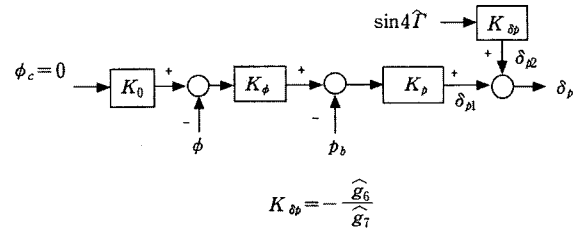


Fig. 4. Roll autopilot structure.

In Fig. 4., ϕ is the roll angle, and $\Delta \phi$ and Δp_b satisfy the following equation.

$$\Delta \dot{\phi} = \Delta p_b \quad (55)$$

Based on Eqs. (54) and (55), K_p, K_ϕ can be determined easily for given trim conditions. Thereafter, K_p and K_ϕ can be scheduled by the Mach number and height, and K_{δ_p} is scheduled by Mach number, height, and total angle of attack. A nonlinear term $K_{\delta_p} \sin 4\hat{\Gamma}$ compensates for the induced roll moment.

3. Integrated flight control system

The block diagram of integrated autopilot is shown in Fig. 5. According to the block diagram, the guidance commands a_{yco} and a_{zco} are transformed to a_{yc} and a_{zc} by the roll angle, first. Then, the autopilot assumed to be fixed in the maneuver coordinates calculates the control fin deflections $(\delta_p, \delta_\rho, \delta_\sigma)$ using the estimates $\hat{\Gamma}$ and \hat{a}_i , and measured outputs from sensors. Finally, $(\delta_p, \delta_\rho, \delta_\sigma)$ are transformed to the actual fin deflections $(\delta_x, \delta_y, \delta_z)$ using the estimate $\hat{\Gamma}_c$.

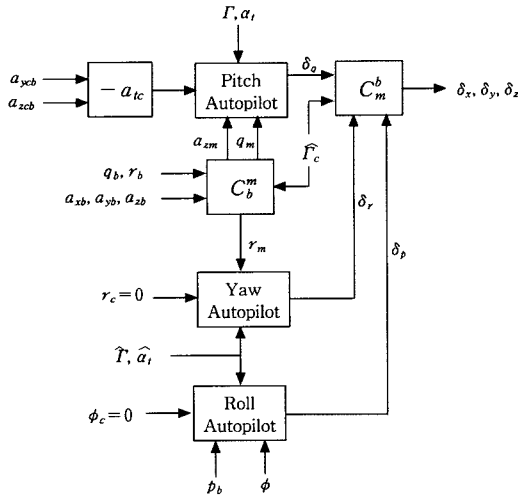
The measured outputs a_{zb}, a_{yb}, q_b and r_b ought to be transformed to the maneuver coordinates via the transform matrix $C_b^m = [-\hat{\Gamma}_c]_X$ before used in each autopilot.

Now, we introduce another structure shown in Fig. 5-b named Structure II. It is worth examining how closely Structure II can approximate the other, because Structure II is much simpler than the other from the viewpoint of implementation. In order to do so, the yaw rate feedback loop should be the same as the pitch rate feedback loop. Then the following procedure seems pertinent to the goal. First, design the linear control part of the autopilot in the body frame without concerning of aerodynamic nonlinearities and induced moments. Next, calculate the compensation terms in the body coordinates by proper transformation, i.e.,

$$\Delta \delta_x = K_{\delta_r} \sin 4\hat{\Gamma}$$

$$\begin{bmatrix} \Delta \delta_y \\ \Delta \delta_z \end{bmatrix} = [-\hat{\Gamma}]_X \begin{bmatrix} K_{\delta_r} \sin 4\hat{\Gamma} \\ K_{\delta_q} \sin 4\hat{\Gamma} \end{bmatrix}$$

So far, it is not quite clear that structure II can be a good substitute in any practical situation, but simulation results, which will be given later, show that the responses of the two structures are very close. It needs further study to make clear the relation between them.



$$C_m^b = [\hat{T}_c]_X, \quad C_b^m = [-\hat{T}_c]_X, \quad a_{tc} = \sqrt{a_{ycb}^2 + a_{zcb}^2}$$

Fig. 5-a. Integrated autopilot(Structure I).

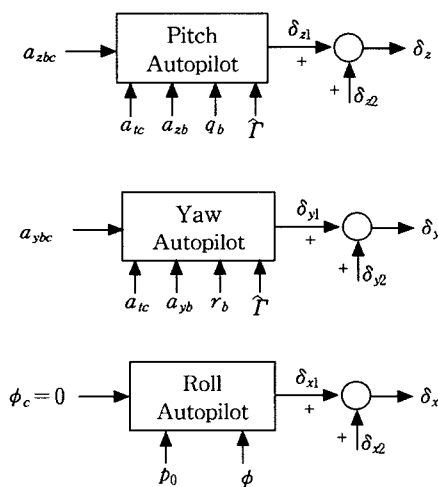


Fig. 5-b. Integrated autopilot(Structure II).

V. Design results and performance analysis about the linearized model

In this section, we explain the design results of the pitch, yaw, and roll autopilot. First, linear control part was designed at the following trim conditions: glide phase, Mach 2.6, bank angle of 22.5°, and total acceleration of 10, 20, 30g. In order to see the effects of aerodynamic nonlinearities and induced moments, we performed two set of linear simulations at bank angles of 0° and 45° using the autopilot designed at the bank angle of 22.5°. The time responses of the first set which has no compensation terms are shown in Fig. 6 and Fig. 7. The responses vary with acceleration command and bank angle severely.

The response of the second set which has compensation

terms is shown in Fig 8. As expected, the effects of nonlinearities and induced moments varying with the bank angle were compensated properly. The responses for other acceleration commands almost same with Fig. 8.

Under the assumption that the true value of bank angle and total angle of attack are available and actuator dynamics is modeled as the 1st order system, the stability was examined at the design points using the complete linearized models which are coupled among the pitch, yaw, and roll channel, and involve actuator dynamics. The results of analysis show that gain and phase margins of the pitch autopilot are more than 10dB and 40°, and the stability margin in roll and yaw autopilot also meet the design requirements.

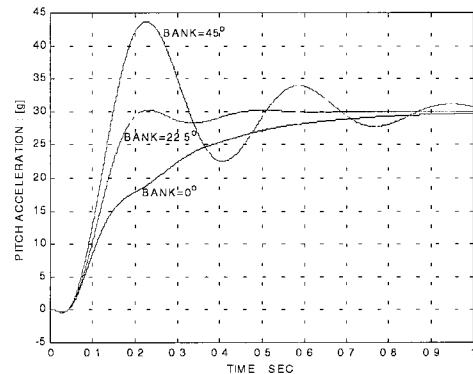


Fig. 6. Responses without compensation term Responses vary with bank angle.

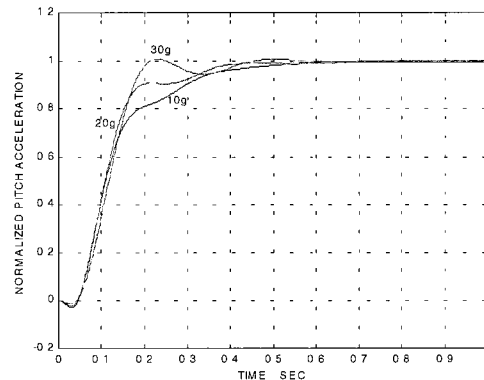


Fig. 7. Responses without compensation terms (bank angle 22.5°). Responses vary with acceleration commands.

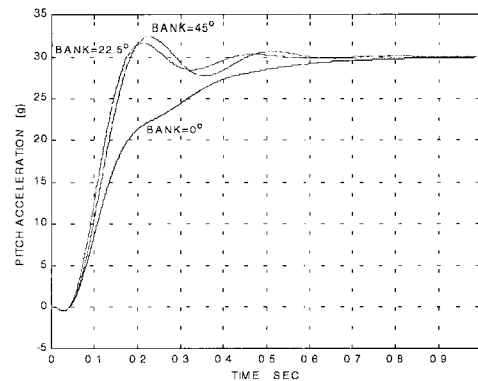


Fig. 8. Responses with compensation terms. The effects of nonlinearities and induced moments varying with the bank angle were compensated.

VI. 6-DOF Simulation

In this section, we show the 6-DOF simulation results. We performed simulations for the 3 cases: Case 1 for an autopilot, which was designed in a conventional way so that no information about bank angle and total angle of attack is used in it, Case 2 and Case 3 for the proposed autopilot with Structure I and Structure II, respectively. For each case, velocity was almost fixed at Mach 2.6 and three kinds of acceleration commands were given so that the bank angle were kept almost at 0°, 22.5°, and 45°, respectively. The results are shown in Fig. 9~12. As expected, Case 2 and Case 3 show superior responses to Case 1. Another notable observation is that Case 2 and Case 3 give very close responses.

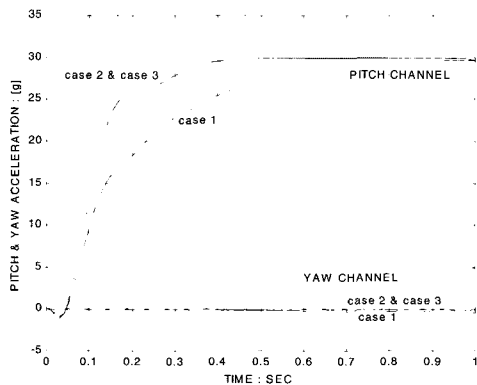


Fig. 9. 6-DOF simulation results.(Pitch and Yaw acceleration, bank angle almost 0°)

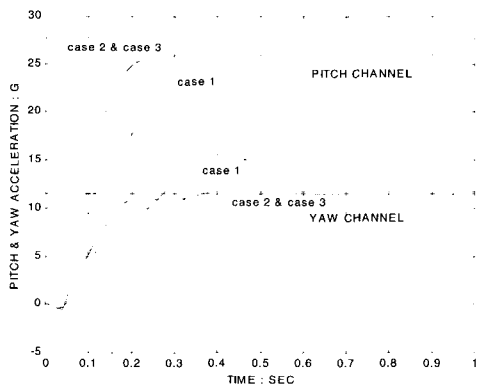


Fig. 10. 6-DOF simulation results.(Pitch and Yaw acceleration, bank angle almost 22.5°)

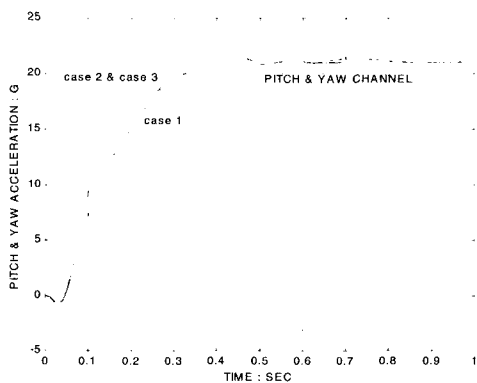


Fig. 11. 6-DOF simulation results.(Pitch and Yaw acceleration, bank angle almost 45°)

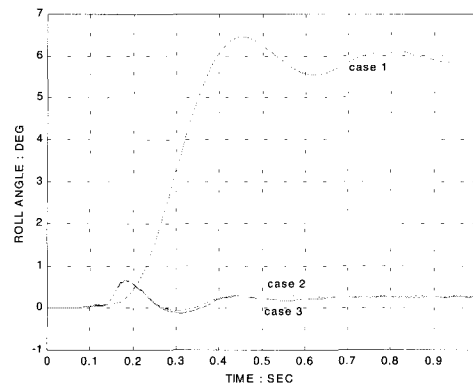


Fig. 12. 6-DOF simulation results.(Roll angle, bank angle almost 22.5°)

VII. Conclusions and further study

A new design approach to the autopilot for STT missiles was proposed. First, we derived the missile motion model where the aerodynamic characteristics are well delineated and based on that model, a design technique for the pitch, yaw, and roll autopilot was presented. With the proposed autopilot and simple estimators of bank angle and total angle of attack, it was shown by computer simulations that the performance is superior to that of the conventional ones.

Robustness problem over the whole closed loop system containing estimators of bank angle and total angle of attack, aerodynamic uncertainties or external disturbances was not considered here. We leave it to future study. We took gain-scheduling scheme to cover the wide range of flight conditions, but analytical gain scheduling studied by Huang and Lin[8] or pseudo-linearization method might give better solution to this problem. As mentioned in the earlier section, Structure II of the proposed autopilot needs further study. Moreover, the structure of linear control part which came from Nesline's work could be extended to more general one. These problems should be addressed in a future study.

References

- [1] M. J. Hemsch, J. N. Nielsen, *Tactical Missile Aerodynamics, Chap. 1*, vol. 104 Progress in Astronautics and Aeronautics, AIAA Inc., 1986.
- [2] A. Arrow and D. J. Yost, "Large angle-of-attack control concepts for aerodynamically controlled missiles," *Journal of Spacecraft*, vol. 14, no. 10, pp. 606-613, 1977.
- [3] J. H. Blakelock, *Automatic Control of Aircraft and Missiles*, John Wiley & Sons, Inc., 1991.
- [4] F. J. Regan, *Re-Entry Vehicle Dynamics*, AIAA Education Series, AIAA Inc., New York, 1984.
- [5] K. R. Britting, *Inertial Navigation Systems Analysis*, John Wiley & Sons Inc., 1971.
- [6] Y. H. Oh, "Three dimensional Interpolation method for missile aerodynamics," *AIAA paper 89-0481, 27th Aerospace Science Meeting, Reno, Nevada*, Jan. 1989.
- [7] F. W. Nesline and M. L. Nesline, "How autopilot requirements constrain the aerodynamic design of homing missiles," *ACC Proc.*, pp. 716-730, 1984.

- [8] J. Huang, C. F. Lin, "Flight control design By nonlinear servomechanism theory," *ACC Proc.*, pp. 410-414, 1993.



Chanho Song

He was born in Seoul, Korea, in 1953. He received B.S. and M.S. degree in Electrical Engineering from Seoul National University in 1975 and 1977, and the Ph.D. degree from University of Florida in 1989, respectively. Since 1977, he has been working as principal

engineer for Agency for Defense Development. His research field includes control theory and guidance and control of missile systems.



Yoon-Sik Kim

He was born in Jinhae, Korea, in 1961. He received B.S., M.S. and ph.D. degrees in Electronic Engineering from Sungkyunkwan University in 1984, 1986 and 2000, respectively. Since 1986 he has been working as senior engineer for Agency for Defense Development.

His research interests are in the areas of guidance and control of missile systems and control application to engineering problem.